JCI The Journal of Clinical Investigation

Atrial fibrillation risk loci interact to modulate Ca^{2+}-dependent atrial rhythm homeostasis

Brigitte Laforest, … , Christopher R. Weber, Ivan P. Moskowitz

J Clin Invest. 2019;129(11):4937-4950. https://doi.org/10.1172/JCI124231.

Research Article **Cardiology** **Genetics**

Atrial fibrillation (AF), defined by disorganized atrial cardiac rhythm, is the most prevalent cardiac arrhythmia worldwide. Recent genetic studies have highlighted a major heritable component and identified numerous loci associated with AF risk, including the cardiogenic transcription factor genes *TBX5*, *GATA4*, and *NKX2-5*. We report that *Tbx5* and *Gata4* interact with opposite signs for atrial rhythm controls compared with cardiac development. Using mouse genetics, we found that AF pathophysiology caused by *Tbx5* haploinsufficiency, including atrial arrhythmia susceptibility, prolonged action potential duration, and ectopic cardiomyocyte depolarizations, were all rescued by *Gata4* haploinsufficiency. In contrast, *Nkx2-5* haploinsufficiency showed no combinatorial effect. The molecular basis of the TBX5/GATA4 interaction included normalization of intra-cardiomyocyte calcium flux and expression of calcium channel genes *Atp2a2* and *Ryr2*. Furthermore, GATA4 and TBX5 showed antagonistic interactions on an *Ryr2* enhancer. Atrial rhythm instability caused by *Tbx5* haploinsufficiency was rescued by a decreased dose of phospholamban, a sarco/endoplasmic reticulum Ca^{2+}-ATPase inhibitor, consistent with a role for decreased sarcoplasmic reticulum calcium flux in *Tbx5*-dependent AF susceptibility. This work defines a link between *Tbx5* dose, sarcoplasmic reticulum calcium flux, and AF propensity. The unexpected interactions between *Tbx5* and *Gata4* in atrial rhythm control suggest that evaluating specific interactions between genetic risk loci will be necessary for ascertaining personalized risk from genetic association data.

Atrial fibrillation risk loci interact to modulate Ca^{2+}-dependent atrial rhythm homeostasis

Brigitte Laforest,[1] Wenli Dai,[2] Leonid Tyan,[3] Sonja Lazarevic,[1] Kaitlyn M. Shen,[1] Margaret Gadek,[1] Michael T. Broman,[3] Christopher R. Weber,[2] and Ivan P. Moskowitz[1,2]

[1]Department of Pediatrics, Pathology, and Human Genetics, [2]Department of Pathology, and [3]Department of Medicine, University of Chicago, Chicago, Illinois, USA.

Atrial fibrillation (AF), defined by disorganized atrial cardiac rhythm, is the most prevalent cardiac arrhythmia worldwide. Recent genetic studies have highlighted a major heritable component and identified numerous loci associated with AF risk, including the cardiogenic transcription factor genes *TBX5*, *GATA4*, and *NKX2-5*. We report that *Tbx5* and *Gata4* interact with opposite signs for atrial rhythm controls compared with cardiac development. Using mouse genetics, we found that AF pathophysiology caused by *Tbx5* haploinsufficiency, including atrial arrhythmia susceptibility, prolonged action potential duration, and ectopic cardiomyocyte depolarizations, were all rescued by *Gata4* haploinsufficiency. In contrast, *Nkx2-5* haploinsufficiency showed no combinatorial effect. The molecular basis of the TBX5/GATA4 interaction included normalization of intra-cardiomyocyte calcium flux and expression of calcium channel genes *Atp2a2* and *Ryr2*. Furthermore, GATA4 and TBX5 showed antagonistic interactions on an *Ryr2* enhancer. Atrial rhythm instability caused by *Tbx5* haploinsufficiency was rescued by a decreased dose of phospholamban, a sarco/endoplasmic reticulum Ca^{2+}-ATPase inhibitor, consistent with a role for decreased sarcoplasmic reticulum calcium flux in *Tbx5*-dependent AF susceptibility. This work defines a link between *Tbx5* dose, sarcoplasmic reticulum calcium flux, and AF propensity. The unexpected interactions between *Tbx5* and *Gata4* in atrial rhythm control suggest that evaluating specific interactions between genetic risk loci will be necessary for ascertaining personalized risk from genetic association data.

Introduction

Atrial fibrillation (AF) is the most common sustained cardiac arrhythmia, affecting more than 7 million Americans and 33 million people worldwide (1). AF is characterized by an irregular pattern of atrial depolarization, resulting in rapid and disorganized atrial conduction and lack of effective atrial chamber contraction. The rhythm abnormality in patients with AF manifests with circulatory deficits and systemic thromboembolism that greatly increase morbidity and mortality. Because age is an independent risk factor for AF, its prevalence is expected to rise significantly as the population ages. AF has become a major clinical and economic burden, owing to the limitations and side effects associated with current AF therapies. Although AF most often manifests in the context of pre-existing cardiac pathologies, such as hypertension and cardiomyopathy, idiopathic or lone AF forms have indicated a heritable component (2). Genome-wide association studies (GWAS) have to date identified more than 100 AF-associated loci, including many transcription factor (TF) loci, suggesting that transcriptional control of atrial rhythm is an important mediator of AF risk (3, 4).

Recent work has illuminated a role for abnormal cardiomyocyte calcium (Ca^{2+}) handling in the cellular pathophysiology of AF. The current paradigm of AF causation describes ectopic (triggered) atrial activity, mediated by early and delayed afterdepolarization (EAD and DAD) events and a fibrillogenic substrate that propagates the abnormal triggers causing arrhythmia. EADs and DADs have been associated with abnormal cardiomyocyte Ca^{2+} handling, including RYR2 dysfunction, reduced sarco/endoplasmic reticulum Ca^{2+}-ATPase 2 (SERCA2) (encoded by *ATP2A2*) activity, and/or increased Na^+/Ca^{2+} exchanger (NCX) activity (5–9). It remains to be defined how alterations of *RYR2*, *ATP2A2*, or *NCX* expression in AF models contribute to AF risk.

GWAS and familial inheritance have implicated transcription factor genes in AF pathogenesis, including the cardiogenic transcription factors (TFs) TBX5, GATA4, and NKX2-5 (2, 10). Autosomal dominant mutations in the T-box TF *TBX5* cause Holt-Oram syndrome, characterized by upper limb malformations, congenital heart defects, cardiac conduction system abnormalities, and increased AF risk (11, 12). In addition, GWAS has identified common risk variants associated with PR interval and increased AF susceptibility in intergenic or intronic regions of TBX5 (13–16). Adult-specific *Tbx5* deletion in mice leads to spontaneous and sustained AF, characterized by slowed conduction and decrements in the expression of ion channels linked to AF (17). TBX5 drives the atrial expression of *Pitx2*, and TBX5 and PITX2 comodulate the expression of cardiac rhythm effector genes, including *Ryr2* and *Atp2a2*. These findings indicated that interactions between TBX5 and PITX2 provide tight control of an atrial rhythm gene regulatory network and that perturbation of this network triggered AF susceptibility (17). This example suggested that cardiac TFs implicated in AF by genetic association may coregulate a gene regulatory

Authorship note: CRW and IPM are co–senior authors. BL and WD contributed equally to this work.
Conflict of interest: The authors have declared that no conflict of interest exists.

Submitted: August 14, 2018; **Accepted:** August 16, 2019; **Published:** October 14, 2019.
Reference information: *J Clin Invest*. 2019;129(11):4937–4950.
https://doi.org/10.1172/JCI124231.

network for atrial rhythm homeostasis. GATA4 and NKX2-5 are particularly relevant candidates, given that they both interact physically and genetically with TBX5 during cardiac development. GATA4, a zinc finger transcription factor, plays critical roles in heart development and cardiomyocyte differentiation (18–20). Several *GATA4* loss-of-function mutations have been reported to underlie AF susceptibility in humans (10, 21–23). GATA4 is highly expressed in adult cardiomyocytes; however, its specific role in atrial cardiac rhythm has not been investigated. *NKX2-5*, a homeodomain containing TF has been implicated in AF by GWAS and family studies (13, 24–26). Common variants associated with PR prolongation, a marker for increased AF risk, have also been identified close to *NKX2-5* by GWAS (13). Heterozygous mutations in *NKX2-5* are associated with a spectrum of congenital heart diseases (CHDs) in humans and mice (27–31). NKX2-5 also has been shown to regulate a number of target genes involved in the cardiomyocyte action potential, suggesting that it may play a direct role in AF predisposition (32).

Combinatorial interactions between TBX5, GATA4, and NKX2-5 are critical for heart development. TBX5, GATA4, and NKX2-5 physically interact, and CHD-causing (but not CHD-sparing) mutations in TBX5 abrogate these interactions (33). Mutations in *GATA4* that disrupt transcriptional cooperativity with TBX5 result in CHD and impaired cardiac gene expression, leading to aberrant chromatin states and gene expression (33, 34). *Tbx5/Gata4* double-heterozygous mice develop cardiac defects that are more severe than *Tbx5* or *Gata4* haploinsufficient mice alone, providing evidence for a cooperative interaction (35). TBX5, NKX2-5, and GATA4 synergistically activate multiple cardiac enhancers and promoters (33, 36–45). Cooperative interactions between TBX5, NKX2-5, and GATA4 on cardiac gene expression may rely on interdependent binding of these factors genome-wide, enabling co-regulation of the cardiac differentiation program (46). Removal of *Tbx5* or *Nkx2-5* in mouse embryonic stem cell cardiac differentiations or *GATA4* in human induced pluripotent stem cardiac differentiations resulted in inappropriate distribution of the other TFs to lineage-inappropriate sites, inducing ectopic gene regulation (34, 46). This paradigm suggested that heterotypic interactions between these cardiogenic TFs may influence atrial rhythm control.

We investigated the combinatorial genetic interactions between the cardiogenic transcription factors *Tbx5*, *Gata4*, and/or *Nkx2-5* in murine atrial rhythm control. We hypothesized that adult-specific combined *Tbx5*, *Gata4*, or *Nkx2-5* haploinsufficiency may alter AF susceptibility and illuminate AF pathophysiology. Surprisingly, we found that *Gata4* haploinsufficiency rescued the cardiac rhythm, cardiomyocyte electrophysiology, and molecular defects caused by *Tbx5* haploinsufficiency. In contrast, introducing *Nkx2-5* haploinsufficiency had no observed effect on the penetrance or severity of defects caused by *Tbx5* haploinsufficiency alone. *Gata4* haploinsufficiency rescued the calcium-handling defects and *Ryr2* and *Atp2a2* gene expression deficits caused by *Tbx5* haploinsufficiency. We found that GATA4 negatively modulated TBX5 activation of a *cis*-regulatory element at *Ryr2*. This observation indicated that GATA4 could repress TBX5-dependent transcriptional activation in some contexts and provided a molecular model for the rescue of *Tbx5* haploinsufficiency by *Gata4* haploinsufficiency. We tested the hypothesis that rescue of *Tbx5* haploinsufficiency was mediated by rescue of calcium homeostasis. Introduction of haploinsufficiency for phospholamban (Pln), a SERCA inhibitor, into *Tbx5*-haploinsufficient mice caused normalization of cardiac rhythm and rescue of SERCA activity. Rescue of the *Tbx5*-haploinsufficient phenotype by *Gata4* deficiency illuminated a TF genetic interaction in atrial rhythm control and provided a molecular model for transcriptional control of cardiomyocyte calcium flux as a central component of atrial rhythm homeostasis.

Results

Reduced Gata4 rescues atrial arrhythmias caused by reduced Tbx5. We previously demonstrated that adult-specific *Tbx5* deletion or haploinsufficiency caused spontaneous AF or AF susceptibility, respectively, linking TBX5 dose with AF risk (17). GATA4 and NKX2-5 physically and genetically interact with TBX5 during cardiac development, and all 3 cardiogenic TFs are strongly expressed in the adult atrium and are genetically linked to AF risk in humans (Figure 1A and refs. 2, 33, 35, 41, 46–48). We therefore hypothesized that GATA4 and NKX2-5 would genetically interact with TBX5 in adult atrial rhythm control. We employed a conditional knockout strategy to establish haploinsufficiency of *Gata4*, *Tbx5*, and *Nkx2-5* singly or in combination in the adult mouse, affording normal gene dosage throughout development to circumvent early lethality or structural heart defects observed with each mouse model (43, 49–51). We combined TF floxed alleles ($Gata4^{fl/fl}$; or $Tbx5^{fl/fl}$ or $Nkx2\text{-}5^{fl/fl}$) with a tamoxifen (TM)-inducible *Cre* recombinase allele at the Rosa26 locus ($R26^{CreERT2}$) to generate adult compound haploinsufficient *Gata4/Tbx5* ($Gata4^{fl/+};Tbx5^{fl/+};R26^{CreERT2}$), *Gata4/Nkx2-5* ($Gata4^{fl/+};Nkx2\text{-}5^{fl/+};R26^{CreERT2}$), *Tbx5/Nkx2-5* ($Tbx5^{fl/+};Nkx2\text{-}5^{fl/+};R26^{CreERT2}$), and triple-haploinsufficient ($Tbx5^{fl/+};Gata4^{fl/+};Nkx2\text{-}5^{fl/+};R26^{CreERT2}$) mice (28, 43, 52). All TF allelic combinations were generated and evaluated as littermates in a mixed genetic background. Mice were treated with TM at 6 weeks of age and loss of *Gata4*, *Tbx5*, and/or *Nkx2-5* expression was confirmed in the left atrium by qPCR 2 weeks following TM treatment (Figure 1B and Supplemental Figure 1A; supplemental material available online with this article; https://doi.org/10.1172/JCI124231DS1). Specifically, *Gata4* decrements were not observed in *Tbx5* or *Nkx2-5* single heterozygotes, indicating that TBX5 or NKX2-5 alone does not regulate expression of *Gata4* (Figure 1B and Supplemental Figure 1A). Similarly, *Tbx5* (or *Nkx2-5*) expression is not regulated by GATA4 or NKX2-5 (or TBX5) alone. However, a greater reduction in *Gata4* expression was observed in *Tbx5/Nkx2-5* compound heterozygotes compared with their respective single-haploinsufficient controls ($P = 0.195$ vs $Tbx5^{fl/+};R26^{CreERT2}$, $P = 0.038$ vs $Nkx2\text{-}5^{fl/+};R26^{CreERT2}$, respectively), suggesting that TBX5 and NKX2-5 may cooperatively regulate GATA4.

We first confirmed that atrial rhythm was sensitive to *Tbx5* dosage in these mixed-background crosses by examining adult *Tbx5* heterozygotes ($Tbx5^{fl/+};R26^{CreERT2}$). Significant prolongation of the *P*-wave duration representing atrial depolarization (AF-associated finding in human studies) was observed in $Tbx5^{fl/+};R26^{CreERT2}$ mice compared with control littermates 2 weeks after TM treatment by conscious ambulatory telemetry ECG ($P = 0.0008$) (Figure 1C and Supplemental Table 1). The PR interval, representing the period between initiation of atrial and ventricu-

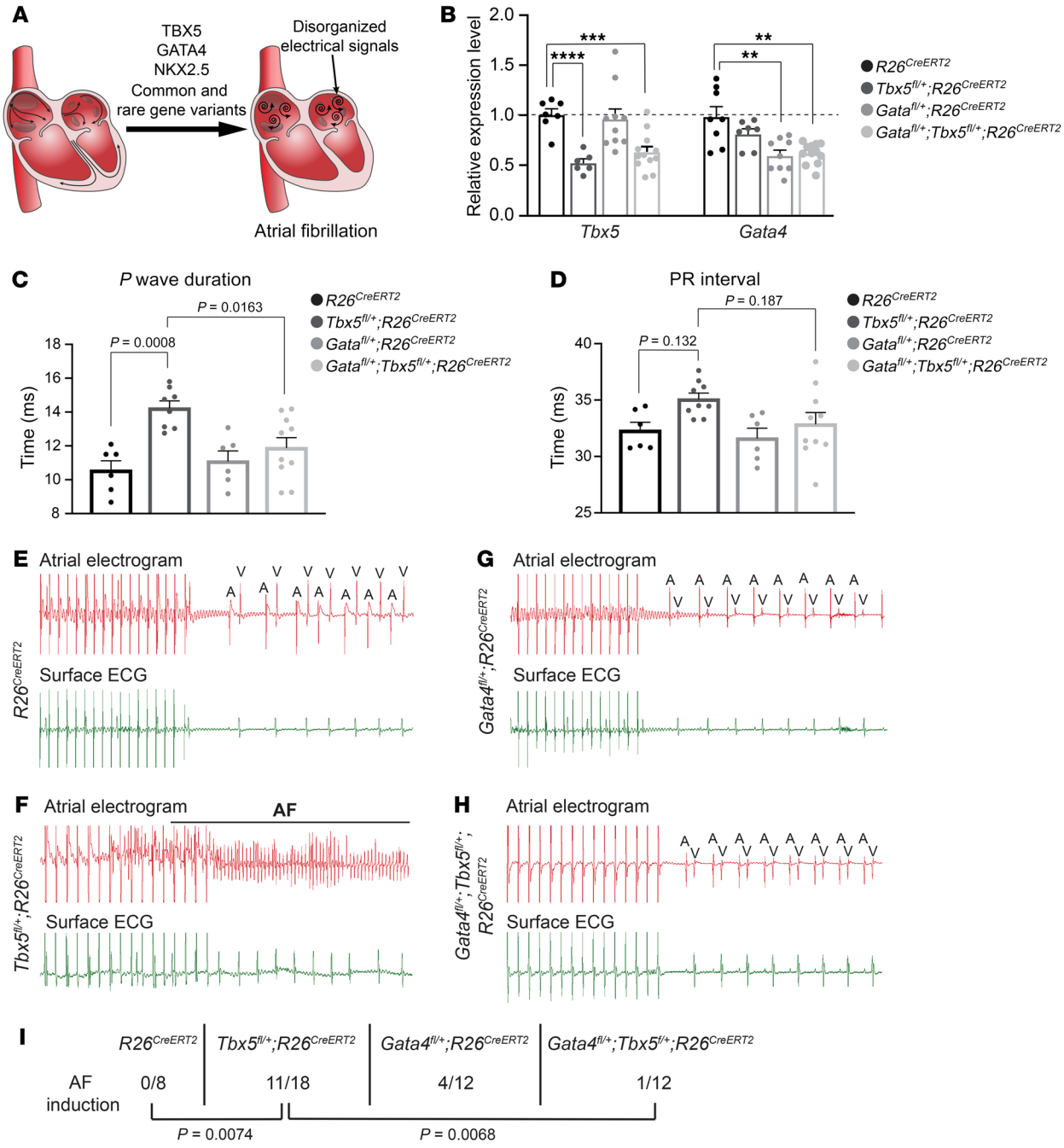

Figure 1. *Gata4* haploinsufficiency rescues atrial arrhythmias caused by *Tbx5* haploinsufficiency. (**A**) Common and rare gene variants in the transcription factors *TBX5*, *GATA4*, and *NKX2-5* have been linked to increased AF susceptibility. (**B**) Relative transcript expression by qPCR in the left atrium of $Tbx5^{fl/+};R26^{CreERT2}$, $Gata4^{fl/+};R26^{CreERT2}$, and *Gata4/Tbx5* compound heterozygotes 2 weeks after TM treatment. Data are represented as means ± SEM normalized to GAPDH and relative to $R26^{CreERT2}$ mice (set as 1) (n = 7–8 $R26^{CreERT2}$, n = 6–7 $Tbx5^{fl/+};R26^{CreERT2}$, n = 9–10 $Gata4^{fl/+};R26^{CreERT2}$, n = 12 $Gata4^{fl/+};Tbx5^{fl/+};R26^{CreERT2}$). Experiments were performed in technical duplicates. P values were determined by 1-way ANOVA followed by Tukey post-hoc test. $^{**}P$ = 0.01; $^{***}P$ = 0.001; $^{****}P$ = 0.0001. (**C** and **D**) P-wave duration and PR interval calculated from ambulatory telemetry ECG recordings from $R26^{CreERT2}$ (n = 6), $Tbx5^{fl/+};R26^{CreERT2}$ (n = 8–9), $Gata4^{fl/+};R26^{CreERT2}$ (n = 6), and $Gata4^{fl/+};Tbx5^{fl/+};R26^{CreERT2}$ (n = 10) mice. $Tbx5^{fl/+};R26^{CreERT2}$ adult mice displayed significant increase in P-wave duration (**C**) and prolongation of the PR interval compared with $R26^{CreERT2}$ littermate controls (**D**). P values were determined by 1-way ANOVA followed by post-hoc Tukey test. (**E**–**H**) Intracardiac atrial electrogram recordings and corresponding surface ECG of $R26^{CreERT2}$ (n = 8), $Tbx5^{fl/+};R26^{CreERT2}$ (n = 18), $Gata4^{fl/+};R26^{CreERT2}$ (n = 12), and $Gata4^{fl/+};Tbx5^{fl/+};R26^{CreERT2}$ (n = 12) mice. *Tbx5* heterozygotes displayed an irregular atrial electrogram, consistent with lack of P wave on surface ECG, which is representative of AF (**F**). A, atrial electrical signal; V, far-field ventricular electrical signal. (**I**) Pacing induction by intra-atrial pacing of mice in **D**–**G**. AF was reproducibly induced in 11 of 18 *Tbx5* heterozygotes (60%) in contrast to 1 of 12 *Gata4/Tbx5* compound heterozygotes, indicating rescue of atrial arrhythmias. P values were determined by Fisher's exact test.

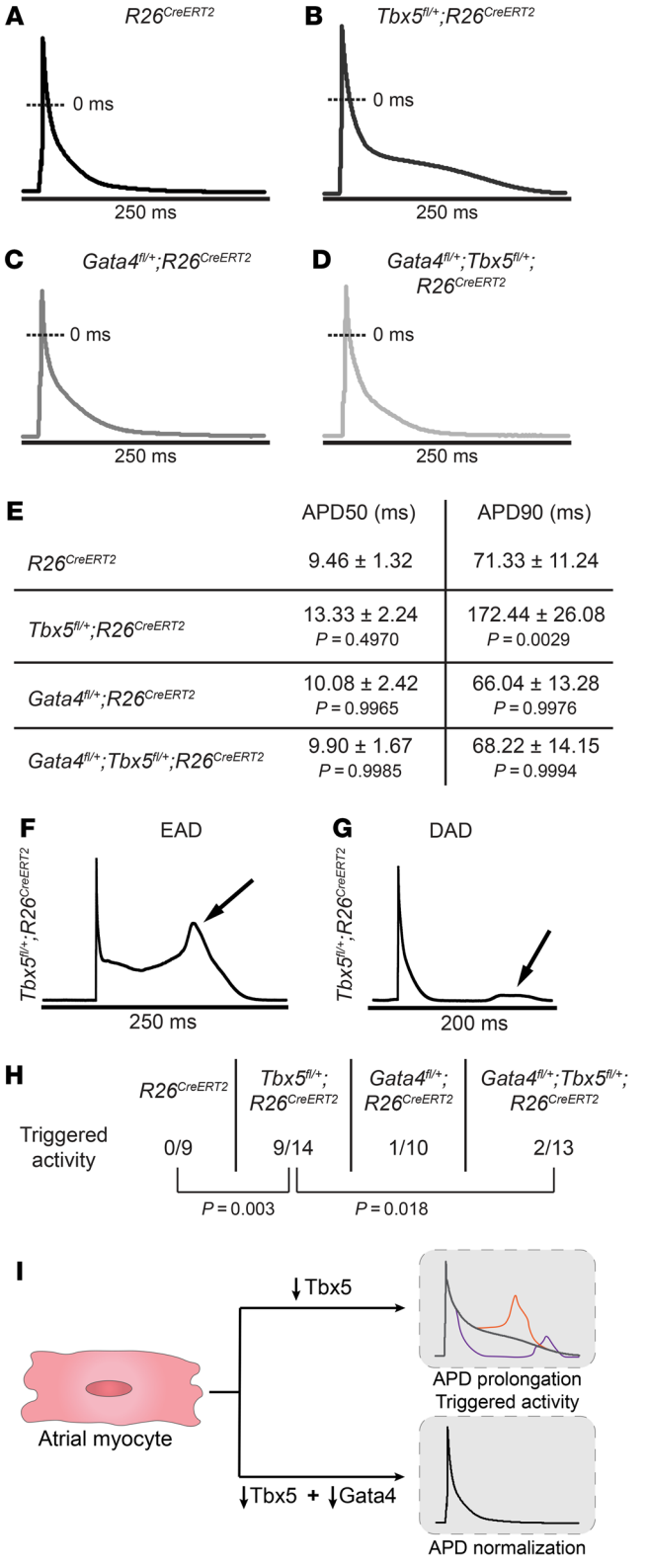

Figure 2. Abnormal atrial cardiomyocyte electrical activity caused by *Tbx5* haploinsufficiency is rescued by *Gata4* haploinsufficiency. (**A**–**D**) Representative AP recordings from atrial myocytes isolated from $R26^{CreERT2}$, $Tbx5^{fl/+};R26^{CreERT2}$, $Gata4^{fl/+};R26^{CreERT2}$, and $Gata4^{fl/+};Tbx5^{fl/+};R26^{CreERT2}$ mice 2 weeks after receiving TM. Prolongation of phase 2 and 3 of the AP was observed exclusively in $Tbx5^{fl/+};R26^{CreERT2}$ mice (**B**) but not in $Gata4^{fl/+};Tbx5^{fl/+};R26^{CreERT2}$ littermates (**D**), suggesting rescue of AP abnormalities. (**E**) Corresponding properties of AP from mice in **A**–**D**. *Tbx5* heterozygotes showed significant prolongation of APD90 in comparison with $R26^{CreERT2}$ controls. These defects were completely rescued in *Gata4/Tbx5* compound heterozygote mice (APD90, $P = 0.006$). APD50, APD at 50% repolarization; APD90, APD at 90% repolarization. Data represent mean ± SEM (n = 3–5 animals per genotype; n = 9 cardiomyocytes $R26^{CreERT2}$, n = 14 $Tbx5^{fl/+};R26^{CreERT2}$, n = 10 $Gata4^{fl/+};R26^{CreERT2}$, and n = 13 $Gata4^{fl/+};Tbx5^{fl/+};R26^{CreERT2}$). P values of APD50 and APD90 were determined by 1-way ANOVA followed by Tukey post-hoc test. (**F** and **G**) Representative tracings of EADs and DADs in $Tbx5^{fl/+};R26^{CreERT2}$ atrial myocytes. (**H**) Representative abnormal depolarization events (EADs and DADs) observed in atrial myocytes. Reduced *Gata4* gene dosage rescued abnormal triggers observed in *Tbx5*- haploinsufficient atrial myocytes. Total number of ectopic depolarization events were recorded in $R26^{CreERT2}$ (n = 9), $Tbx5^{fl/+};R26^{CreERT2}$ (n = 14), $Gata4^{fl/+};R26^{CreERT2}$ (n = 10), and $Gata4^{fl/+};Tbx5^{fl/+};R26^{CreERT2}$ (n = 13) atrial myocytes from $n > 4$ for each genotype. P values of triggers were determined by Fisher's exact test. (**I**) The cellular conduction deficits caused by *Tbx5* haploinsufficiency, including AP prolongation and triggered activity and normalization by reduced *Gata4* dose.

lar depolarization, was unchanged in $Tbx5^{fl/+};R26^{CreERT2}$ compared with $R26^{CreERT2}$ mice ($P = 0.132$) (Figure 1D and Supplemental Table 1), consistent with our previous publication (17). We further interrogated propensity to atrial arrhythmias by catheter-directed intracardiac pacing. $Tbx5^{fl/+};R26^{CreERT2}$ adult mice were highly susceptible to AF induction, depicted by the irregular atrial electrogram, by intracardiac atrial pacing using either programmed single extra-stimulus or burst pacing. AF was reproducibly induced in 11 of 18 $Tbx5^{fl/+};R26^{CreERT2}$ mice but in 0 of 8 $R26^{CreERT2}$ mice following atrial burst pacing ($P = 0.0074$) (Figure 1, E, F, and I). Of these, 7 of 11 $Tbx5^{fl/+};R26^{CreERT2}$ mice displayed atrial tachycardia (AT) and/or AF episodes lasting greater than 1,000 ms ($P = 0.0128$), with a mean duration of 15,963 ms. In addition, 4 of 11 *Tbx5* heterozygotes ($P = 0.103$) displayed rapid atrial irregular rhythm for less than 1,000 ms, with a mean duration of 678 ms. Remarkably, 5 of 11 $Tbx5^{fl/+};R26^{CreERT2}$ mice displayed spontaneous atrial arrhythmias in addition to induced irregular atrial rhythm (Supplemental Figure 2). $Tbx5^{fl/+};R26^{CreERT2}$ mice showed normal cardiac function 2 weeks after TM treatment, with no difference in left ventricular ejection fraction compared with $R26^{CreERT2}$ adult mice (Supplemental Figure 3). These findings establish that *Tbx5* haploinsufficiency causes atrial conduction deficits and increased AF risk.

Atrial rhythm was not sensitive to adult-specific *Gata4* or *Nkx2-5* haploinsufficiency. Adult-specific *Gata4* ($Gata4^{fl/+};R26^{CreERT2}$) or *Nkx2-5* ($Nkx2\text{-}5^{fl/+};R26^{CreERT2}$) haploinsufficiency caused no abnormalities of *P*-wave duration ($P = 0.928$ $R26^{CreERT2}$ vs $Gata4^{fl/+};R26^{CreERT2}$ and $P = 0.08$ $R26^{CreERT2}$ vs $Nkx2\text{-}5^{fl/+};R26^{CreERT2}$) or PR interval ($P = 0.956$ $R26^{CreERT2}$ vs $Gata4^{fl/+};R26^{CreERT2}$ and $P = 0.985$ $R26^{CreERT2}$ vs $Nkx2\text{-}5^{fl/+};R26^{CreERT2}$) by conscious ambulatory telemetry ECG and showed no sign of beat-to-beat variability by Poincaré analysis in comparison with $R26^{CreERT2}$ control littermates ($P = 0.946$ $R26^{CreERT2}$ vs $Gata4^{fl/+};R26^{CreERT2}$ and $P = 0.992$ $R26^{CreERT2}$ vs $Nkx2\text{-}5^{fl/+};R26^{CreERT2}$) (Figure 1, C and D, Supplemental Figure 1, and Supplemental Table 1). Unlike reduced *Tbx5* dosage, *Gata4* or *Nkx2-5* haploinsufficient mice were not vulnerable to atrial arrhythmias by pacing induction (Figure 1, F, G, and I, and Supplemental Figure 4). Specifically, 4 of 12 $Gata4^{fl/+};R26^{CreERT2}$ mice ($P = 0.116$) and 1 of 8 $Nkx2\text{-}5^{fl/+};R26^{CreERT2}$ mice ($P = 0.5$) experienced AF compared with 0 of 9 $R26^{CreERT2}$ mice and both showed sta-

tistically less AF inducibility than *Tbx5* haploinsufficiency (P = 0.0074) (Figure 1, G and I, and Supplemental Figure 4B).

Remarkably, atrial arrhythmicity caused by reduced *Tbx5* dose was rescued by reduced *Gata4* dose. Specifically, the increased *P*-wave duration observed in *Tbx5*-haploinsufficient mice was rescued in combined *Gata4/Tbx5*-haploinsufficient mice (P = 0.0163 *Gata4/Tbx5*- compound heterozygote versus $Tbx5^{fl/+};R26^{CreERT2}$) (Figure 1C). *Gata4/Tbx5*-compound heterozygotes were not susceptible to AF induction by intracardiac burst pacing. Only 1 of 12 $Gata4^{fl/+};Tbx5^{fl/+};R26^{CreERT2}$ mice reproducibly paced into AF, demonstrating rescue of AF inducibility compared with 11 of 18 for $Tbx5^{fl/+};R26^{CreERT2}$ mice (P = 0.0068) and no greater propensity for AF induction compared with $R26^{CreERT2}$ controls (0 of 8 $R26^{CreERT2}$, P = 0.999) (Figure 1, H and I).

Nkx2-5 haploinsufficiency had no discernable effect on atrial rhythm, by itself or in combination with *Tbx5* or *Gata4* haploinsufficiency. We analyzed adult-specific *Tbx5/Nkx2-5* and *Gata4/Nkx2-5* compound heterozygotes and *Gata4/Tbx5/Nkx2-5* triple heterozygotes for atrial conduction deficits or arrhythmia inducibility. No significant *P*-wave duration or PR interval differences were detected in any of these genotypes compared with their respective single- or double- haploinsufficient controls (Supplemental Figure 1, B and C, and Supplemental Table 1). Furthermore, no significant differences in atrial arrhythmia inducibility were observed in *Gata4/Nkx2-5* (P = 0.999 vs $Gata4^{fl/+};R26^{CreERT2}$ and P = 0.999 vs $Nkx2\text{-}5^{fl/+};R26^{CreERT2}$) or *Tbx5/Nkx2-5* ($P$ = 0.361 vs $Tbx5^{fl/+};R26^{CreERT2}$ and P = 0.323 vs $Nkx2\text{-}5^{fl/+};R26^{CreERT2}$) compound heterozygotes compared with their respective single- heterozygote controls or in *Gata4/Tbx5/Nkx2-5* triple heterozygotes compared with *Gata4/Tbx5* double-heterozygote controls (P = 0.999) (Supplemental Figure 4). Specifically, 1 of 12 $Gata4^{fl/+};Nkx2\text{-}5^{fl/+};R26^{CreERT2}$ mice paced into AF compared with control littermates, suggesting that GATA4 and NKX2-5 do not interact together in the adult heart for control of atrial rhythm (Supplemental Figure 4, D and F). $Tbx5^{fl/+};Nkx2\text{-}5^{fl/+};R26^{CreERT2}$ mice were susceptible to AF induction by intracardiac burst pacing, with prevalence identical to that of *Tbx5* heterozygotes, indicating that TBX5 and NKX2-5 do not interact synergistically or antagonistically in the adult atrium (Supplemental Figure 4, C and F). Finally, mice lacking 1 copy of *Gata4*, *Tbx5*, and *Nkx2-5* ($Tbx5^{fl/+};Gata4^{fl/+};Nkx2\text{-}5^{fl/+};R26^{CreERT2}$) were not vulnerable to AF induction (Supplemental Figure 4, E and F). Thus, the AF susceptibility observed in *Tbx5/Nkx2-5* compound heterozygotes was rescued by reducing *Gata4* gene dosage, similar to $Tbx5^{fl/+};Gata4^{fl/+};R26^{CreERT2}$ mice. In each genetic context, *Nkx2-5* was dispensable, causing no worsening or improvement of atrial rhythm in adult mice compared with littermate controls.

Abnormal atrial electric activity observed in Tbx5 heterozygotes is normalized in Gata4/Tbx5 compound heterozygotes. We sought to define the cellular basis by which reduced *Gata4* dose rescued the atrial conduction deficits and arrhythmia propensity caused by reduced *Tbx5* dose. We previously showed that adult-specific *Tbx5* haploinsufficiency caused prolonged atrial cardiomyocyte (CM) action potentials (APs) and abnormal spontaneous depolarizations of atrial myocytes, electrophysiological deficits that can cause or contribute to AF (17). We hypothesized that *Gata4* haploinsufficiency may rescue the cellular electrophysiology defects caused by *Tbx5* haploinsufficiency. APs from atrial myocytes isolated from $Tbx5^{fl/+};R26^{CreERT2}$ mice 2 weeks after TM treatment were significantly prolonged, specifically in phases 2 and 3 of the AP and time to 90% repolarization (APD90), compared with $R26^{CreERT2}$ atrial myocytes (P = 0.0029) (Figure 2, A, B, and E, and Supplemental Table 2). EADs and DADs were frequently observed in $Tbx5^{fl/+};R26^{CreERT2}$ atrial myocytes but never in control littermates (9 of 14 $Tbx5^{fl/+};R26^{CreERT2}$ vs 0 of 9 $R26^{CreERT2}$ atrial myocytes, P = 0.003), consistent with our previous study (Figure 2, F–H, and ref. 17). Adult-specific *Gata4* haploinsufficiency caused no aberrations in AP measurements or inappropriate afterdepolarizations (Figure 2, C, E, and H, and Supplemental Table 2). Remarkably, decreased *Gata4* dose rescued the cellular electrophysiology abnormalities observed in $Tbx5^{fl/+};R26^{CreERT2}$ mice. Atrial AP duration was rescued in $Gata4^{fl/+};Tbx5^{fl/+};R26^{CreERT2}$ myocytes (P = 0.0006) (Figure 2, B, D, and E). Additionally, propensity of EADs and DADs was rescued in $Gata4^{fl/+};Tbx5^{fl/+};R26^{CreERT2}$ compared with $Tbx5^{fl/+};R26^{CreERT2}$ atrial myocytes (P = 0.018), and $Gata4^{fl/+};Tbx5^{fl/+};R26^{CreERT2}$ atrial myocytes showed no increased propensity for inappropriate depolarizations compared with $R26^{CreERT2}$ control atrial myocytes (P = 0.493) (Figure 2H). We conclude that the cellular electrophysiology defects caused by decreased *Tbx5* dose were rescued by reduced *Gata4* dose (Figure 2I).

Atrial myocyte ectopic activity, implicated as a mechanism of AF induction, can result from abnormal calcium handling. We therefore investigated altered expression of genes controlling cardiomyocyte calcium flux as a potential molecular mechanism for paroxysmal AF induction in *Tbx5* heterozygote mice. We focused on calcium-handling genes involved in phase 2 and 3 of the AP, given our observation of specific deficits during these AP phases in *Tbx5* adult haploinsufficient mice (Figure 2). Adult-specific *Tbx5* heterozygote mice showed significantly diminished left atrial expression of *Atp2a2* and *Ryr2* compared with $R26^{CreERT2}$ mice (P = 0.0038 for *Atp2a2*; P = 0.0163 for *Ryr2*, respectively), whereas expression of other calcium-handling genes, including *Sln*, *Pln*, *Slc8a1*, and *Cacna1c* were not significantly altered (Figure 3A and Supplemental Table 3). Interestingly, *Atp2a2* and *Ryr2* expression was normalized in *Gata4/Tbx5* compound heterozygotes (P = 0.0232 for *Atp2a2*; P = 0.0323 for *Ryr2*, respectively) (Figure 3A and Supplemental Table 3). In addition, we also assessed expression of potassium-handling genes previously linked to AF. RNA expression of *Kcnj3* (P = 0.0443), *Kcnj5* (P = 0.0039), and *Kcnh2* (P = 0.0182) showed significant reduction in left atrial tissue of $Tbx5^{fl/+};R26^{CreERT2}$ mice compared with control littermates (Supplemental Figure 5), whereas expression of *Kcna5*, *Kcnd3*, *Kcnk2*, *Kcnn3*, and *Kcnq1* were unchanged. However, *Kcnj3*, *Kcnj5*, or *Kcnh2* gene expression was not normalized in $Gata4^{fl/+};Tbx5^{fl/+};R26^{CreERT2}$ mice (P = 0.7001 for *Kcnj3*, P = 0.4254 for *Kcnj5* and P = 0.5286 for *Kcnh2*, respectively). Overall, these results suggested that atrial arrhythmogenesis in adult *Tbx5* heterozygous mice may be mediated by altered sarcoplasmic reticulum (SR) calcium flux, mediated by reduced expression of *Atp2a2* and *Ryr2*.

We previously demonstrated that TBX5 drives atrial expression of *Pitx2* and that TBX5 and PITX2 oppositely modulate the expression of cardiac rhythm effector genes, including *Ryr2* and *Atp2a2* (17). This finding suggested that the rescue of *Tbx5* haploinsufficiency by Gata4 haploinsufficiency could occur through diminished *Pitx2* levels. *Pitx2* mRNA expression remained unchanged

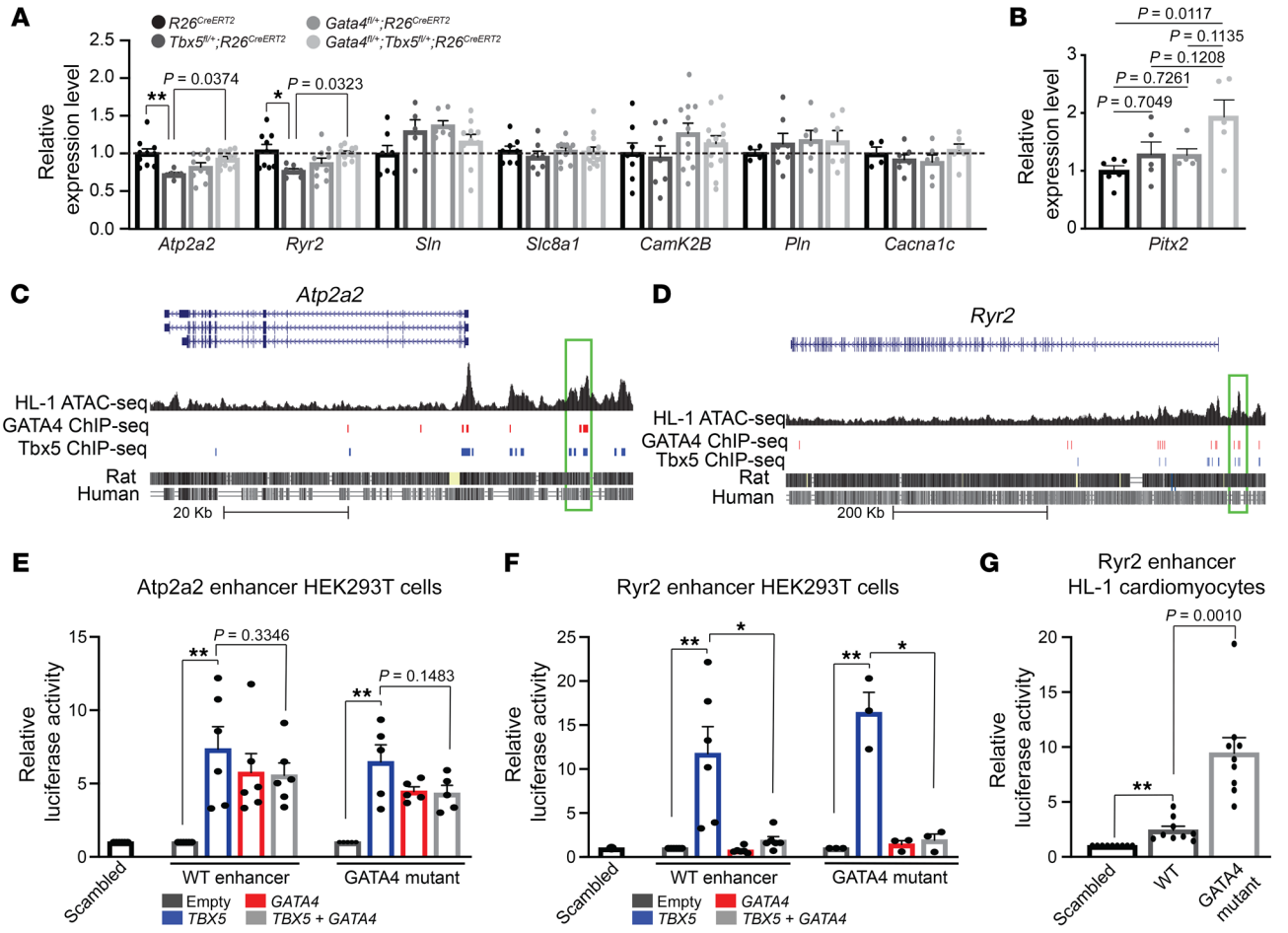

Figure 3. Antagonistic interactions between TBX5 and GATA4 on *Atp2a2* and *Ryr2* expression and on an *Ryr2* enhancer. (**A**) Relative gene expression by qPCR of known AF calcium genes and calcium-interacting proteins from left atrium of $R26^{CreERT2}$ (n = 6–10) $Tbx5^{fl/+};R26^{CreERT2}$ (n = 5–7), $Gata4^{fl/+};R26^{CreERT2}$ (n = 7–10), and $Gata4^{fl/+};Tbx5^{fl/+};R26^{CreERT2}$ (n = 9–13) mice 2 weeks after TM treatment. *Tbx5* heterozygotes showed 20% decrease in *Atp2a2* and *Ryr2* gene expression, which was normalized in *Gata4/Tbx5* compound heterozygotes. Data are normalized to GAPDH and relative to $R26^{CreERT2}$. *P* values were determined by 1-way ANOVA followed by Tukey post-hoc test. (**B**) Relative transcript expression of *Pitx2* by qPCR in the left atrium of *Tbx5* heterozygotes, *Gata4* heterozygotes, and *Gata4/Tbx5* compound heterozygotes 2 weeks after TM treatment. Data are represented as means ± SEM normalized to GAPDH and relative to $R26^{CreERT2}$ mice (set as 1) (n = 6 $R26^{CreERT2}$, n = 5 $Tbx5^{fl/+};R26^{CreERT2}$, n = 5 $Gata4^{fl/+};R26^{CreERT2}$, and n = 5 $Gata4^{fl/+};Tbx5^{fl/+};R26^{CreERT2}$). Experiments were performed in technical duplicates. *P* value was determined by 1-way ANOVA followed by post-hoc Tukey test. (**C** and **D**) *Atp2a2* and *Ryr2* genomic locus (Mm9) aligned with published ATAC-seq dataset from HL-1 cardiomyocytes and ChIP-seq dataset for TBX5 and GATA4. Green rectangle denotes the cis-regulatory regions with overlapping open chromatin as well as TBX5- and GATA4-binding motifs. (**E**–**G**) In vitro luciferase response assay of *Atp2a2* and *Ryr2* candidate enhancers in HEK293T cells cotransfected with TBX5 and/or GATA4 or HL-1 atrial cardiomyocytes and corresponding GATA mutant enhancer. Data are means ± SEM, normalized to scrambled vector. Experiments were performed in technical triplicates (n = 5 for *Atp2a2* enhancer; n = 4 for *Ryr2* in HEK293T cells and n = 5 for *Ryr2* in HL-1 cardiomyocytes). *P* values were determined by 1-way ANOVA followed by Tukey post-hoc test. $^*P < 0.05$; $^{**}P < 0.01$.

in $Tbx5^{fl/+};R26^{CreERT2}$ and $Gata4^{fl/+};R26^{CreERT2}$ mice 2 weeks after TM treatment, as previously described (P = 0.7049 $Tbx5^{fl/+};R26^{CreERT2}$ compared with $R26^{CreERT2}$ and P = 0.7261 $Gata4^{fl/+};R26^{CreERT2}$ compared with $R26^{CreERT2}$) (Figure 3B and ref. 17). Levels of *Pitx2* mRNA were slightly higher in $Gata4^{fl/+};Tbx5^{fl/+};R26^{CreERT2}$ mice compared with WT littermates (P = 0.0117); however, this increase was not significant compared with $Tbx5^{fl/+};R26^{CreERT2}$ or $Gata4^{fl/+};R26^{CreERT2}$ mice (P = 0.1208 vs $Tbx5^{fl/+};R26^{CreERT2}$ and P = 0.1135 vs $Gata4^{fl/+};R26^{CreERT2}$ mice, respectively). This observation suggested that the rescue of *Tbx5* haploinsufficiency by *Gata4* haploinsufficiency was not mediated by a reduction of *Pitx2* expression.

We hypothesized that TBX5 and GATA4 directly coregulate expression of *Atp2a2* and *Ryr2*. To test this hypothesis, we defined regions with overlapping chromatin occupancy for both TBX5 and GATA4 from published ChIP datasets (Figure 3, C and D, Supplemental Figures 6 and 7, and ref. 53). Candidate cis-regulatory elements (CREs) were refined by open chromatin regions from the HL-1 cardiomyocyte ATAC-seq dataset (54). We functionally interrogated these CREs for enhancer activity in the presence of TBX5 and/or GATA4. The *Atp2a2* enhancer (mm9 Chr5: 122970476-122971591) demonstrated activation in response to *TBX5* expression in human embryonic kidney (HEK) 293T cells, as previously described (Figure 3E and ref. 54). *GATA4* similarly activated the enhancer and coexpression of TBX5, and GATA4 had no additive or synergistic effects by in vitro luciferase reporter assay in HEK293T cells (Figure 3E). In contrast, the *Ryr2* enhancer was activated by TBX5 (P = 0.0013) but not GATA4 alone (P = 0.5923) in HEK293T cells (Figure 3F). Remarkably, co-expression

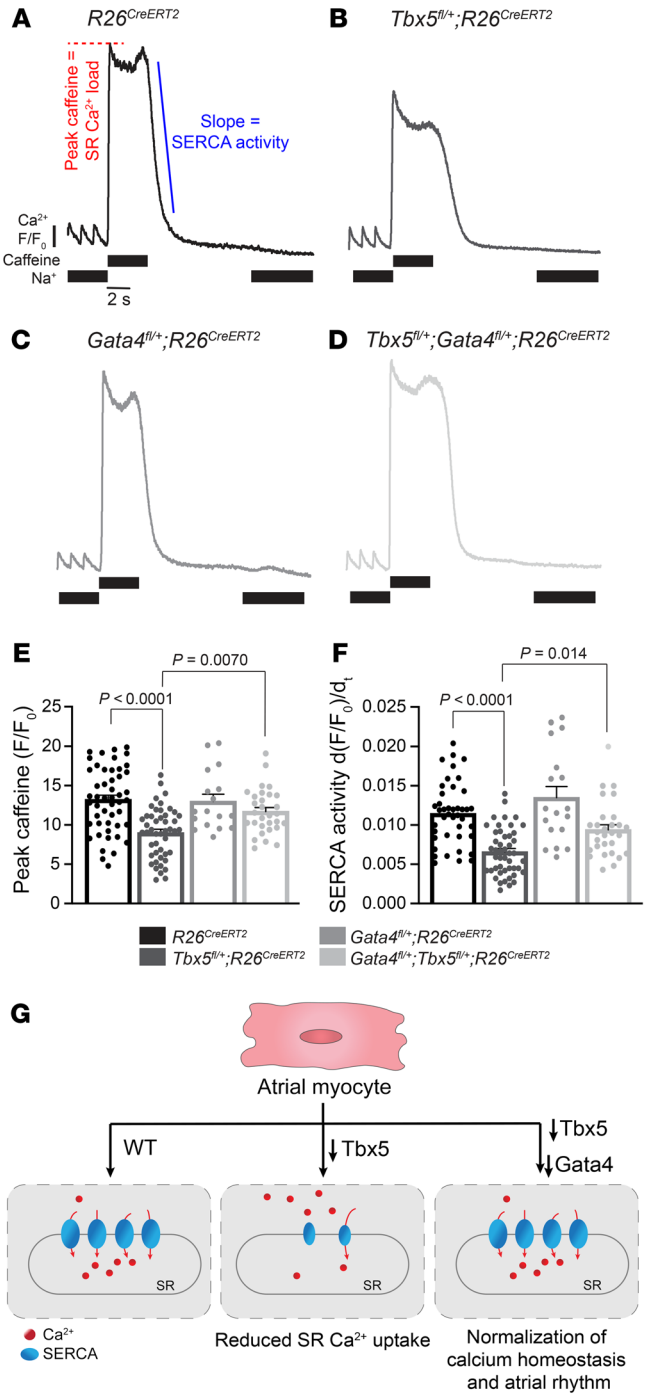

Figure 4. Reduced SERCA function caused by *Tbx5* haploinsufficiency is rescued by *Gata4* haploinsufficiency in atrial myocytes. (**A**–**D**) Representative SERCA2 traces after steady-state field stimulation at 1 Hz and application of caffeine in the absence of Na_o provides a measurement of SR load. Removal of caffeine in the absence of external Nao provides a measure of SERCA2-mediated SR calcium uptake. (**E**) SR load, determined from peak caffeine transients was diminished in $Tbx5^{fl/+};R26^{CreERT2}$ compared with $R26^{CreERT2}$ mice and was completely rescued in $Gata4^{fl/+};Tbx5^{fl/+};R26^{CreERT2}$ mice (n = 49 $R26^{CreERT2}$, n = 47 $Tbx5^{fl/+};R26^{CreERT2}$, n = 18 $Gata4^{fl/+};R26^{CreERT2}$ and n = 30 $Gata4^{fl/+};Tbx5^{fl/+};R26^{CreERT2}$ atrial myocytes from 3–5 mice for each genotype). P values were determined by 1-way ANOVA followed by post-hoc Tukey test. (**F**) SERCA activity determined from the maximal rate of calcium decay was diminished in $Tbx5^{fl/+};R26^{CreERT2}$ compared with $R26^{CreERT2}$ and normalized by *Gata4* haploinsufficiency. P values were determined by 1-way ANOVA followed by post-hoc Tukey test. (**G**) Calcium homeostasis in control atrial myocytes is disrupted by *Tbx5* haploinsufficiency and rescued by decreasing *Gata4* gene dosage.

of GATA4 suppressed TBX5-dependent transactivation of this *Ryr2* enhancer (P = 0.0681 compared with TBX5 alone), suggesting antagonistic interactions of TBX5 and GATA4 on this CRE. We further tested the *Ryr2* CRE in HL-1 cardiomyocytes, which possesses expression of cardiac transcription factors, including TBX5 and GATA4 (55). This enhancer previously demonstrated TBX5-dependent activity in HL-1 cells, and consistently, this enhancer alone showed activation in HL-1 cardiomyocytes (Figure 3G and ref. 54). Interestingly, mutation of the 4 GATA binding motifs within this enhancer caused an increase of enhancer activity in HL-1 cardiomyocytes (P = 0.0010 vs WT enhancer) (Figure 3G). These observations indicated that GATA4 represses TBX5-dependent activity of the *Ryr2* enhancer.

Reduced SR load and SERCA function caused by Tbx5 haploinsufficiency is rescued by Gata4 haploinsufficiency. Abnormal CM membrane depolarizations, including DADs, can be induced by Ca^{2+}-driven Na^+/Ca^{2+} exchanger (NCX) activity in the setting of reduced SERCA-mediated SR Ca^{2+} uptake, causing membrane depolarization (56). We therefore hypothesized that the ectopic depolarizations caused by *Tbx5* haploinsufficiency would be associated with depressed SERCA function and slowed SR Ca^{2+} uptake. To test this hypothesis, we measured SR load and SERCA activity in *Tbx5* heterozygote atrial myocytes, 2 weeks after TM treatment. We used nonfluorescent acetoxymethyl ester (Fluo-4 AM) to study cytosolic calcium-handling kinetics and Fura-2 acetoxymethyl ester (Fura-2 AM) to study diastolic calcium levels. We defined SR Ca^{2+} uptake by loading myocytes with Fluo-4 AM and pacing with a train-of-field stimuli to achieve a steady-state load followed by application of caffeine to synchronize ryanodine receptor opening, resulting in a maximum release of SR calcium into the cytosol (Figure 4, A–D). We observed reduced caffeine-induced calcium-transient amplitudes in $Tbx5^{fl/+};R26^{CreERT2}$ in comparison with $R26^{CreERT2}$ mice, indicating reduced SR calcium levels (P < 0.0001) (Figure 4, A, B, and E). To assess SERCA activity, we measured $[Ca]_i$ decay rate after caffeine in the absence of external sodium (NCX inactive), allowing measurement of isolated SR uptake. Consistent with reduced left atrial expression of *Atp2a2*, we observed decreased SERCA activity in *Tbx5*-haploinsufficient mice (P < 0.0001) (Figure 4, A, B, and F, and Supplemental Figure 8). Furthermore, no significant differences were observed in resting cytosolic calcium between $Tbx5^{fl/+};R26^{CreERT2}$ and $R26^{CreERT2}$ cardiomyocytes (1.001 $Tbx5^{fl/+};R26^{CreERT2}$ vs 0.992 $R26^{CreERT2}$, P = 0.515) (Supplemental Figure 8). This finding suggests that the observed differences in SERCA function are not due to alterations in cytosolic calcium levels or calcium buffering capacity, but rather to TBX5-depedent regulation of SERCA. Overall, our findings indicate that *Tbx5* haploinsufficiency causes reduced SERCA function, providing a molecular mechanism for ectopic CM depolarizations (Figure 4G).

Decreased *Gata4* dose rescued abnormal SERCA function observed in *Tbx5*-haploinsufficient mice. Specifically, SR calcium load in $Gata4^{fl/+};Tbx5^{fl/+};R26^{CreERT2}$ myocytes was not different

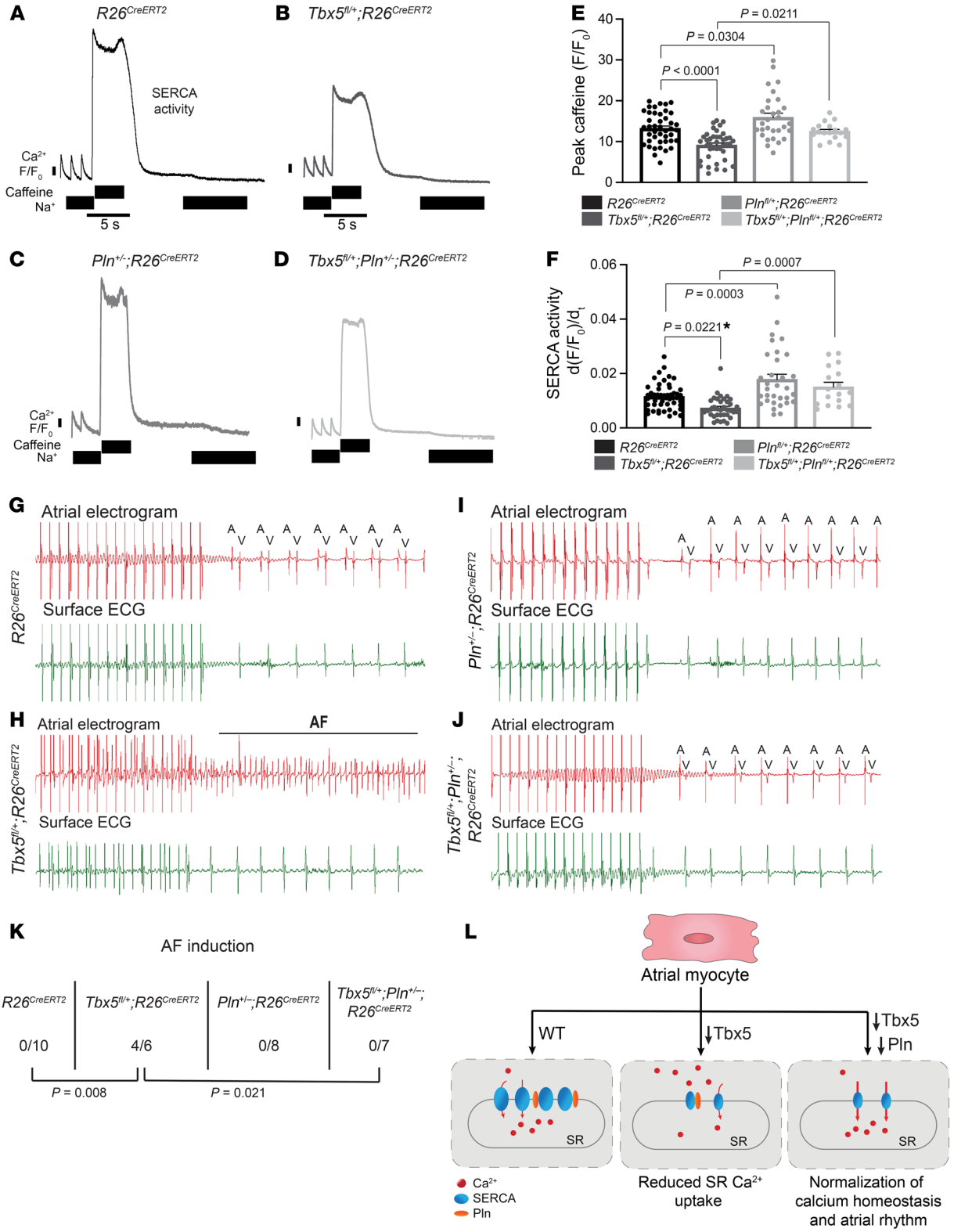

Figure 5. Normalization of SERCA2 function eliminates AF susceptibility in *Tbx5*$^{fl/+}$;*R26*^{CreERT2}. (**A**–**D**) Representative SERCA2 traces of *R26*^{CreERT2} (**A**), *Tbx5*$^{fl/+}$;*R26*^{CreERT2} (**B**), *Pln*$^{+/-}$;*R26*^{CreERT2} (**C**), and *Tbx5*$^{fl/+}$;*Pln*$^{+/-}$;*R26*^{CreERT2} (**D**) atrial myocytes. (**E** and **F**) Representative SR load and SERCA2 measurements from **A**–**D**. SR load (**E**) and SERCA2 function (**F**) was low in *Tbx5*$^{fl/+}$;*R26*^{CreERT2} and normalized in *Tbx5/Pln* compound heterozygous mice (n = 43 *R26*^{CreERT2}, n = 40 *Tbx5*$^{fl/+}$;*R26*^{CreERT2}, n = 30 *Pln*$^{+/-}$;*R26*^{CreERT2}, and n = 18 *Tbx5*$^{fl/+}$;*Pln*$^{+/-}$;*R26*^{CreERT2}) For SR load and SERCA2 measurements, 3–4 mice per genotype were analyzed. (**G**–**J**) Intracardiac atrial electrogram recordings and corresponding surface ECG of *R26*^{CreERT2} (n = 9), *Tbx5*$^{fl/+}$;*R26*^{CreERT2} (n = 6), *Pln*$^{+/-}$;*R26*^{CreERT2} (n = 8), and *Pln*$^{+/-}$;*Tbx5*$^{fl/+}$;*R26*^{CreERT2} (n = 7) mice. *Tbx5* heterozygotes displayed irregular atrial electrogram, representative of AF (**H**). A, atrial electrical signal; V, far-field ventricular electrical signal. (**K**) Pacing induction by intra-atrial pacing of mice in **G**–**J**. AF was reproducibly induced in 4 of 6 *Tbx5* heterozygotes (60%) in contrast to 0 of 7 *Pln/Tbx5* compound heterozygotes, indicating complete rescue of atrial arrhythmias. *P* values were determined by Fisher's exact test; *P < 0.05. (**L**) Calcium homeostasis in control atrial myocytes is disrupted by *Tbx5* haploinsufficiency and rescued by decreasing *Pln* gene dosage.

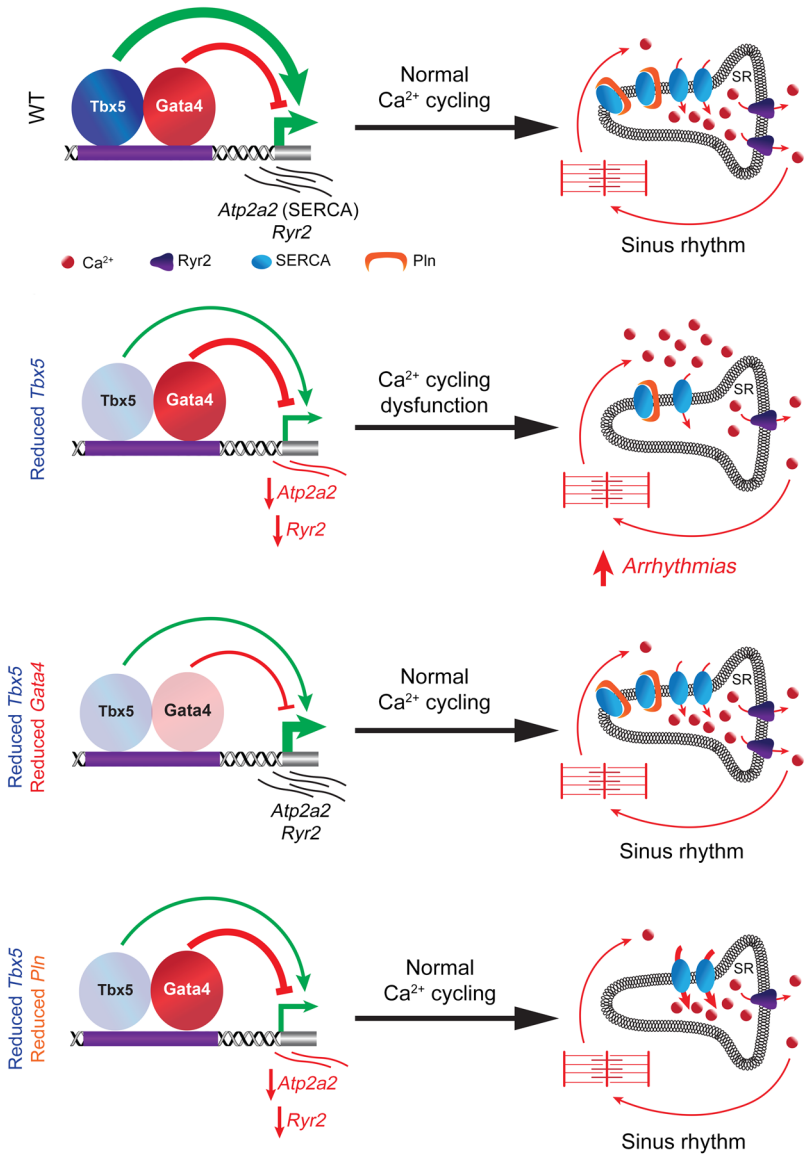

Figure 6. TBX5 and GATA4 are key regulators of atrial calcium homeostasis. Proteins involved in Ca^{2+} handling of atrial myocytes. In the healthy atrium, calcium homeostasis is maintained through a tight balance between Ca^{2+} fluxes across the membrane. Reducing *Tbx5* gene dosage in the adult heart results in depressed *Atp2a2* expression and SERCA2 function, affecting SR Ca^{2+} influx. Abnormal Ca^{2+} handling leads to Ca^{2+} accumulation in the cytosol, contributing to ectopic atrial activity, prolonged APs, and atrial arrhythmias observed with adult-specific *Tbx5* haploinsufficiency. Reducing *Gata4* gene dosage rescues *Atp2a2* expression, SERCA2 function and SR Ca^{2+} uptake, restoring sinus rhythm. SERCA2 and its inhibitory protein PLN play a fundamental role in Ca^{2+} handling within atrial myocytes. Reducing *Pln* gene dosage, as a means to modulate SERCA2 function, normalizes SERCA2 activity and SR Ca^{2+} uptake, resulting in restoration of sinus rhythm in combined *Tbx5/Pln* haploinsufficiency.

from $R26^{CreERT2}$ control cardiomyocytes ($P = 0.312$), and $Gata4^{fl/+};Tbx5^{fl/+};R26^{CreERT2}$ myocytes showed a significantly increased SR load compared with $Tbx5^{fl/+};R26^{CreERT2}$ cardiomyocytes ($P = 0.0070$) (Figure 4, B, D, and E). Furthermore, SERCA activity was normalized in $Gata4^{fl/+};Tbx5^{fl/+};R26^{CreERT2}$ myocytes as observed by a normal decay rate upon removal of caffeine, compared with $Tbx5^{fl/+};R26^{CreERT2}$ cardiomyocytes ($P = 0.0145$) (Figure 4, B, D, and F). Additional analysis of the calcium dependence of SERCA activity showed decreased activity at all levels of cytosolic calcium in $Tbx5^{fl/+};R26^{CreERT2}$ compared with $R26^{CreERT2}$, and this was normalized in $Gata4^{fl/+};Tbx5^{fl/+};R26^{CreERT2}$ mice (Supplemental Figure 8). We conclude that the atrial calcium homeostasis defects caused by reduced *Tbx5* dose were rescued by reduced *Gata4* dose, providing a molecular mechanism for the physiological rescue (Figure 4G).

Modulation of SERCA function eliminates TF-driven arrhythmogenic phenotype. The observation that reduced *Gata4* dose rescued the defects caused by a reduced *Tbx5* dose at the level of cardiac rhythm control, cellular electrophysiology, gene expression, and reduced SR calcium flux suggested that the pathophysiology of reduced *Tbx5* dose on atrial rhythm control may be entirely mediated by reduced SR calcium uptake.

PLN inhibits SERCA activity in its nonphosphorylated state. *Pln* is essential for atrial calcium homeostasis, and human genetic variants at *PLN* associate with AF risk, suggesting that PLN activity contributes to AF susceptibility (3, 57). We hypothesized that reducing *Pln* gene levels may restore SERCA activity and rescue atrial calcium abnormalities caused by reduced *Tbx5* dose. We compared SR uptake, SERCA function, and AF inducibility in adult-specific littermate *Tbx5*-haploinsufficient, *Pln*-haploinsufficient or *Tbx5/Pln* double-haploinsufficient mice 2 weeks after TM treatment. We observed depressed SR load ($P < 0.0001$) and SERCA activity ($P = 0.0221$) in atrial cardiomyocytes from $Tbx5^{fl/+};R26^{CreERT2}$ mice compared with those from $R26^{CreERT2}$ littermate controls, as expected (Figure 5, A, B, E, and F). *Pln* heterozygote atrial cardiomyocytes showed a significant increase in SR load ($P = 0.0304$) and SERCA function ($P = 0.0003$) compared with those from $R26^{CreERT2}$ (Figure 5, A, C, E, and F). Both SR load ($P = 0.0211$) and SERCA activity ($P = 0.0007$) were normalized in *Tbx5/Pln* compound heterozygotes (Figure 5L).

We hypothesized that normalization of SERCA function and SR load in *Tbx5/Pln* compound heterozygotes may rescue the AF predisposition caused by decreased *Tbx5* dose. *Tbx5* heterozygotes were highly susceptible to atrial arrhythmias, consistent with our previous observations (Figure 1, E and H). AF was induced in 4 of 6 $Tbx5^{fl/+};R26^{CreERT2}$ mice compared with 0 of 10 for $R26^{CreERT2}$ controls ($P = 0.008$) (Figure 5, H and K). *Pln* heterozygotes demonstrated no AF inducibility (0 of 8 mice; $P = 0.999$) (Figure 5, I and K). Remarkably, $Tbx5^{fl/+};Pln^{+/-};R26^{CreERT2}$ adult mice were not susceptible to AF induction by intracardiac pacing (0 of 7 $Tbx5^{fl/+};Pln^{+/-};R26^{CreERT2}$ mice; $P = 0.021$ vs $Tbx5^{fl/+};R26^{CreERT2}$) (Figure 5, G–K). Overall, we conclude that decreased *Pln* gene dose

normalizes SERCA activity and rescues AF susceptibility caused by *Tbx5* haploinsufficiency, indicating that diminished SERCA activity is a primary deficit causing arrhythmogenesis in the setting of *Tbx5* haploinsufficiency (Figure 5L).

Discussion

We report that TBX5 and GATA4, both implicated in human AF, genetically interact in mice for atrial rhythm control with unanticipated results. Surprisingly, reducing *Gata4* gene dosage rescued defects caused by *Tbx5* haploinsufficiency, including atrial arrhythmias, prolonged APs, abnormal ectopic cellular depolarizations, SR Ca^{2+} load and SERCA calcium flux. Rescue of both P-wave prolongation and ectopic cardiomyocyte depolarizations suggests that *Gata4* haploinsufficiency may rescue both the vulnerable substrate and arrhythmia trigger propensity caused by *Tbx5* haploinsufficiency. The identification of SERCA function as the nexus of the *Tbx5/Gata4* genetic interaction suggested the more general hypothesis that calcium flux deficits caused by *Tbx5* haploinsufficiency were the primary mechanism for the observed atrial rhythm disturbance. This hypothesis is supported by the ability of the reduced dose of *pln*, encoding a direct-binding SERCA inhibitor, to also rescue the *Tbx5* heterozygote phenotype. By providing insights into the coregulation of atrial rhythm and calcium homeostasis by TBX5 and GATA4, this work illuminates complex genetic interactions that will undergird efforts toward personalized care in human rhythm control. The work also identifies SERCA calcium flux as the pathophysiologic basis of increased AF risk caused by decreased *Tbx5* dose and therefore, a possible pathophysiologic mechanism germane to AF risk more generally.

We defined a calcium-handling network underlying cardiomyocyte prolonged action potentials and ectopy observed with decreased *Tbx5* dose and rescued by reduced *Gata4* dose. We hypothesized that normalization of SERCA expression caused normalization of AP duration and elimination of ectopic depolarization events. Consistently, reduction in *Atp2a2* expression, SERCA activity, and SR Ca^{2+} load observed in *Tbx5* haploinsufficient mice were all rescued by *Gata4* haploinsufficiency (Figure 4). Recent studies investigating the cellular mechanisms of AF have suggested that abnormal atrial calcium handling contributes to AF pathogenesis, leading to trigger formation (56, 58–60). Although SR calcium content is affected by both SERCA uptake and RYR2-mediated calcium leak, our previous study suggested that Ryr2 binding was not affected in *Tbx5* knockout mice, suggesting a primary role of SERCA in TBX5-dependent calcium dysfunction (61). Consistent with this model, increased SERCA activity by reduced PLN, an SERCA inhibitor, rescued the *Tbx5*- haploinsufficient phenotype (Figure 5). Human *PLN* mutations have been previously linked to AF and cardiomyopathy (62–64). Reductions in SERCA2 expression/activity or enhancement of the inhibitory effects of PLN are also hallmarks of heart failure (HF) (65, 66). Interestingly, PLN inhibition has been shown to alleviate cardiomyopathy in several animal models and improve cardiomyocyte contractility in patients with HF (67–69). Here, we show that decreased *Pln* dose can rescue the arrhythmogenic phenotype caused by *Tbx5* haploinsufficiency, by restoring SERCA function and normalizing SR Ca^{2+} content (Figures 4 and 6). Zhu et al. observed rescue of heart failure and ventricular SERCA function following ablation of PLN in *Tbx5*$^{vdel/+}$ mice (70). TBX5 therefore regulates SERCA in both the atria and ventricles for both cardiac function and rhythm. The observation that decreased *Pln* normalizes SR Ca^{2+} uptake and SERCA activity in a mouse model of AF provides a direct molecular link between calcium flux perturbations observed in HF and AF risk, which are strongly associated, regardless of genetic background. These observations suggest that PLN inhibition and more generally, the modulation of SR calcium flux, may be considered as possible therapeutic approaches for the treatment of AF in patients with HF.

Understanding of the genetic basis of cardiac rhythm control has benefited greatly from highly powered genome-wide association studies, which have identified more than 100 loci contributing to the heritability of AF. A mechanistic and actionable understanding of how the identified loci affect cardiac rhythm control requires the transition from genetic implication to functional investigation (71). The implication of the cardiogenic TFs *TBX5, GATA4,* and *NKX2-5* by GWAS is an exciting feature, suggesting a shared transcriptional kernel in cardiac development and adult cardiac rhythm control. In the context of cardiac development, *Tbx5*, *Gata4*, and *Nkx2-5* interact genetically in a synergistic fashion, their encoded TFs physically associate, and they cooperatively drive embryonic cardiac gene expression (33–44). These detailed studies provided a clear paradigm for the cooperative interaction between these TFs in adult rhythm control. Remarkably, we find that these TFs interact very differently in the adult mouse: *Tbx5* and *Gata4* act oppositely, and *Nkx2-5* has no appreciable impact.

Understanding how TBX5 and GATA4 levels are integrated at the molecular level to afford genetic rescue of the *Tbx5* mutant phenotype by reduced *Gata4* activity will be essential for AF risk prediction. We identified an enhancer at *Ryr2* that molecularly integrates GATA4 and TBX5 with opposite activity. Previous work has characterized multiple promoters or enhancers coregulated by TBX5 and GATA4, and in each case, positive interactions were observed, either additive or synergistic (33, 36–41). In a few cases, however, GATA4 has been reported to possess repressive molecular activity on cardiac enhancers. For example, GATA4 recruits Hdac1/2 to deacetylate specific atrioventricular canal loci, thereby repressing AV canal identity during cardiac chamber development (37). GATA4 can also cooperate with -catenin on TCFL2-enhancers in the adult heart, to maintain normal homeostasis through repression of TCFL2-driven loci (72). Therefore, GATA4 harbors repressive potential in some contexts in the heart. Here, we identified a repressive role for GATA4 at an enhancer of *Ryr2*, on which GATA4 opposes TBX5-dependent activation (Figure 3). We observed that TBX5 activation and GATA4 antagonism of the Ryr2 enhancer was dependent on GATA-binding sites in HL-1 cells but not HEK293T cells. One possibility for these different results is the distinct physiological conditions of these cell lines. Because HEK cells lack endogenous expression of TBX5 and GATA4, TF overexpression may overcome the effect of the binding-site mutation because TBX5 and GATA4 physically interact (33). In contrast, HL-1 cells, possessing endogenous physiologic expression of the cardiogenic kernel of TFs, including TBX5 and GATA4, may be more sensitive to the necessity of the GATA binding sites. It remains to be elucidated how GATA4 antagonizes TBX5-dependent function in the adult atrium, perhaps by recruiting repressive chromatin-remodeling enzymes or cardiac corepressors. Nonethe-

less, our observations provide a model for the integration of TBX5 and GATA4 dose on gene expression by the opposite modulation of single- target gene enhancers. Understanding the molecular mechanisms underlying the opposite action of TBX5 and GATA4 on cardiac gene expression will improve our understanding of the molecular basis of adult cardiac rhythm control.

This work unveiled complex genetic interactions between genes individually implicated in AF by human genetic studies. The opposite sign with which decreased *Gata4* dose affected AF risk in the context of decreased *Tbx5* dose indicates the importance of unveiling specific genetic interactions between genetic risk loci for understanding the combined impact of genetic variants across genomes for disease risk prediction. Human genetic studies have been underpowered for the identification of multigenic interactions to date, highlighting the importance of gene-gene interaction studies in model systems such as those included in this study. This work suggests that interaction studies between genetic risk loci will be an essential component of understanding personalized risk from genetic association studies.

Methods

Experimental design. This study was designed to investigate the oligogenic interaction of TFs that have been linked to AF by GWAS studies. We used murine models of conditional *Tbx5* deletion, conditional *Gata4* deletion, conditional *Nkx2-5* deletion, and germline *Pln* heterozygosity for their similarities to human AF phenotypes. The number of mice per genotype depended on the experiments and is specified in figure legends. For animal studies, littermates were used as controls, and mice were grouped when appropriate. Endpoints for studies were selected according the phenotype of adult *Tbx5*-haploinsufficient mice. For single-cell electrophysiology and calcium flux measurements, 3–5 mice per genotype were analyzed, and a total of 10 cells was recorded for every mouse. All experiments, recordings, and analysis were performed in a blinded fashion. Outliers were excluded if samples/replicates were greater than 2 SDs from the population mean.

Transgenic mice. $Tbx5^{fl/fl}$, $Gata4^{fl/fl}$, $Nkx2\text{-}5^{fl/fl}$, $Pln^{+/-}$, and $Rosa\text{-}26^{CreERT2}$ mice have all been previously described (28, 43, 52, 73, 74). Mice were maintained on a mixed genetic background, harboring 1 copy of the Cre recombinase. All experiments involving *Tbx5*, *Gata4*, *NKx2-5*, and *Pln* heterozygotes and *Gata4/Tbx5*, *Tbx5/Nkx2-5*, *Gata4/Nkx2-5*, and *Tbx5/Pln* compound heterozygotes and *Tbx5/Gata4/Nkx2-5* triple heterozygotes were performed 2 weeks after TM treatment, and age-matched littermate controls ($R26^{CreERT2}$) were used for comparison. A total of 200 μl of tamoxifen (20 mg/ml in corn oil) was administered by i.p. injection for 3 consecutive days at 6 to 8 weeks of age, as previously described (17).

Telemetry ECG recordings. Ambulatory ECG studies were performed on 8- to 10-week-old mice. Mice were anesthetized using isoflurane, and telemetry transmitters (ETA-F10, Data Science International [DSI]) were implanted s.c. in the back with leads tunneled to the right upper and left lower thorax, as previously described (75). After the postimplant recovery period of 1 day, baseline recordings were collected by DSI telemetric physiological monitor system. *P*-wave duration, PR interval, and Poincare plots were calculated using Ponemah Physiology Platform (DSI) and custom Python script.

Intracardiac electrophysiology studies. Animals underwent catheter-based intracardiac recordings 2 weeks after receiving TM, as previously described (17). Mice were anesthetized with isoflurane, and right atrial and ventricular electrograms as well as surface electrograms were recorded using a 1.1-F octapolar catheter (EPR-800, Millar Instruments) inserted via the right jugular vein. Programmed extra-stimulation protocols and burst pacing were used to induce AT and AF in animal subjects. Programmed right atrial extra stimulation was carried out using S1 drive trains of 80 ms followed by 5 extra stimulations at 50 ms each. Burst pacing was performed by applying a series of single extra stimulus delivered at a constant pacing rate of 15–20 ppm (900–1200 bpm). Inducibility was considered positive if 2 or more series of AT and/or fibrillation was observed following burst pacing in the same animal. Fibrillation was considered noninducible if 0 or 1 cycle or irregular atrial rhythm was observed in the animal.

Echocardiography. Transthoracic echocardiography was performed 2 weeks after TM treatment under inhaled isoflurane, delivered via a nose cone, as previously described (76). Briefly, animals were imaged with a VisualSonics Vevo 770 machine (VisualSonics) using a 30-MHz high-frequency transducer. Body temperature was maintained using a heated imaging platform. Two-dimensional images were recorded in parasternal long- and short-axis projections, with guided M-mode recordings at the midventricular level in both views. M-mode echocardiographic images were obtained at the midpapillary muscle level in the parasternal short-axis view and measurement calculated at the same level from M- and/or B-mode images of long- or short-axis view. Left ventricular dimensions in both diastole and systole were measured from at least 3 different beats from each projection and averaged to calculate the left ventricular ejection fraction.

Calcium flux measurement. Single-cell atrial cardiomyocytes were isolated by Langendorff perfusion with 2 mg/ml of Collagenase Type 2 at 5 ml/min. Atrial myocytes were plated on laminin-coated glass-bottom dishes and incubated at room temperature for 30 minutes prior to incubation with Fluo-4 AM (Molecular Probes/Invitrogen). Cells were then incubated with 10-μM Fluo-4 AM for 1 hour in normal Tyrode's solution containing (in mM): 140 NaCl, 4 KCl, 10 glucose, 10 HEPES, and 1 $MgCl_2$, 1 $CaCl_2$, with pH 7.4 using NaOH, followed by a 10-minute perfusion wash with pre-warmed Tyrode's solution. SERCA and NCX measurements were performed using an Olympus microscope with a x20 objective lens, a LAMBDA DG-4 power source with 488-nm excitation and 515-nm emission filters and a PMT (Microphotometer) to record whole-cell signal, with electrical field stimulation (Grass stimulator; Astro-Med) at 1 Hz. SERCA and NCX activities were measured as follows: 10-mM caffeine- containing solution was applied in the absence of extracellular sodium and the cells returned to normal Tyrode's solution at the end of the recording. In the presence of sodium-free caffeine Tyrode's solution, the intracellular calcium remains elevated, and the peak value is a measure of SR calcium load that was released into the cytosol.

Whole-cell electrophysiological recordings. Action potentials were recorded using the whole-cell patch-clamp method (17). Whole-cell action potentials were recorded using an Axopatch-200B amplifier connected to a Digidata1550A acquisition system (Axon Instruments). Atrial myocytes were isolated by Langendorff perfusion, plated on laminin-coated glass- bottom dishes and incubated at room temperature for 30 minutes before recordings. Tyrode's solution (140-mM NaCl, 4-mM KCl, 1-mM $MgCl_2$, 1-mM $CaCl_2$, 10-mM HEPES, and 10-mM glucose, pH 7.4 with NaOH) was used to perfuse atrial cardiomyocytes during recordings at 37°C. Internal pipette solution contained 20-mM

KCl, 100-mM K-glutamate, 10-mM HEPES, 5-mM $MgCl_2$, 10-mM NaCl, 5-mM Mg-ATP, and 0.3-mM Na-GTP. Action potentials were triggered using 0.5 nA × 2-ms current clamp pulses following liquid junction potential correction. All recordings were filtered at a frequency of 2 kHz using a built-in Bessel filter and sampled at 10 kHz. Results were analyzed using pCLAMP10 (Axon Instruments).

Diastolic calcium measurements. Atrial myocytes were isolated by Langendorff perfusion, plated on laminin-coated glass-bottom dishes, and incubated at room temperature for 30 minutes before staining with Fura-2 AM. Cells were then incubated with 1-μM Fura-2 AM for 10 minutes in normal Tyrode's solution. Diastolic calcium measurements were performed at a fluorescence emission of 510 nm and recorded using an Olympus IX81 Inverted Widefield Microscope. $[Ca]_i$ was calculated by the ratio of emissions following excitation at 340 nm and 380 nm.

Relative luciferase assays. HEK293T and HL-1 cells were cotransfected as described previously (17). The *Atp2a2* and *Ryr2* cis-regulatory elements were amplified from C57/B6 mouse genomic DNA. The sequence was confirmed by sequencing and then cloned into the pGL4.23 enhancer luciferase response vector with a minimal promoter. Mutagenesis of the GATA4-binding motifs was performed by PCR cloning, confirmed by sequencing and then cloned into the pGL4.23 vector. Cells were co-transfected with the luciferase response vector and pRL control using lipofectamine 3000, then lysed and assayed following 48 hours using the Dual-Luciferase Reporter Assay system (Promega).

Quantitative real-time PCR. Total RNA was extracted from the left atrial wall of 8- to 10-week-old adult mice (2 weeks after receiving TM) using Trizol (Invitrogen) combined with RNeasy mini-kit (Qiagen), according to the manufacturer's instructions. First-strand cDNA was synthesized using the qScript cDNA synthesis kit (Quanta) according to the manufacturer's protocol. Gene expression was assayed using the Power SYBR Green PCR Master Mix (Applied Biosystems) and run on an Applied Biosystems AB7500 machine in 96-well plates. Relative fold changes were calculated using the comparative threshold cycle method ($2^{-\Delta Ct}$) using glyceraldehyde-3-phosphate dehydrogenase (*Gapdh*) as an internal control. Primer sequences used in this study are listed in Supplemental Table 3.

Statistics. All data are represented as means ± SEM. For comparison of conscious ECG parameters, action potential duration (APD50 and APD90), SR load, and SERCA activity, a 1-way ANOVA followed by post-hoc Tukey analysis was used to test significance. For gene-expression studies and in vitro luciferase assays, a 1-way ANOVA followed by internal Student's *t* test was used to test significance. AF inducibility and triggered activity (from AP measurements) counts were analyzed with a Fisher's exact test (2-tailed).

Study approval. All animal experiments were performed in accordance with national and institutional guidelines and were approved by the University of Chicago Institutional Animal Care and Use Committee.

Author contributions

BL and WD were involved in experimental design, execution and analysis, wrote the manuscript, and performed statistical analysis. BL performed and analyzed ambulatory ECG, whole-animal electrophysiology studies, and gene expression. WD performed and analyzed calcium flux measurements. LT performed and analyzed single-cell electrophysiology experiments. SL, KMS, and MG performed and analyzed luciferase assays. MTB performed and analyzed intracardiac electrophysiology studies. CRW performed and analyzed single-cell electrophysiology experiments and wrote the manuscript. IPM was involved in the design, execution, and analysis of experiments and wrote the manuscript.

Acknowledgments

This work was supported by the NIH (R01 HL148719 and R01 HL147571 to IPM; K08HL129073 to MTB), the American Heart Association (7CSA33610126 to IPM) and the Leducq Foundation (to IPM). We thank Evangelia Kranias for the Phospholamban mice (NIH R01 HL26057). This research was supported in part by the NIH through resources provided by the Computation Institute and the Biological Sciences Division of the University of Chicago and Argonne National Laboratory, under grant 1S10OD018495-01.

Address correspondence to: Ivan Moskowitz, University of Chicago, 900 East 57th Street, KCBD Room 5102, Chicago, Illinois 60637, USA. Phone: 773.834.0462; Email: imoskowitz@peds.bsd.uchicago.edu. Or to: Christopher R. Weber, University of Chicago Medicine, 5841 South Maryland Avenue, Room P310, MC1089, Chicago, Illinois 60637, USA. Phone: 773.702.5893; Email: christopher.weber@uchospitals.edu.

1. Nishida K, Datino T, Macle L, Nattel S. Atrial fibrillation ablation: translating basic mechanistic insights to the patient. *J Am Coll Cardiol*. 2014;64(8):823–831.
2. Tucker NR, Ellinor PT. Emerging directions in the genetics of atrial fibrillation. *Circ Res*. 2014;114(9):1469–1482.
3. Roselli C, et al. Multi-ethnic genome-wide association study for atrial fibrillation. *Nat Genet*. 2018;50(9):1225–1233.
4. Nielsen JB, et al. Biobank-driven genomic discovery yields new insight into atrial fibrillation biology. *Nat Genet*. 2018;50(9):1234–1239.
5. Dobrev D, Nattel S. New insights into the molecular basis of atrial fibrillation: mechanistic and therapeutic implications. *Cardiovasc Res*. 2011;89(4):689–691.
6. El-Armouche A, et al. Molecular determinants of altered Ca^{2+} handling in human chronic atrial fibrillation. *Circulation*. 2006;114(7):670–680.
7. Grandi E, et al. Human atrial action potential and Ca^{2+} model: sinus rhythm and chronic atrial fibrillation. *Circ Res*. 2011;109(9):1055–1066.
8. Neef S, et al. CaMKII-dependent diastolic SR Ca^{2+} leak and elevated diastolic Ca^{2+} levels in right atrial myocardium of patients with atrial fibrillation. *Circ Res*. 2010;106(6):1134–1144.
9. Mauritz C, et al. Generation of functional murine cardiac myocytes from induced pluripotent stem cells. *Circulation*. 2008;118(5):507–517.
10. Mahida S, Ellinor PT. New advances in the genetic basis of atrial fibrillation. *J Cardiovasc Electrophysiol*. 2012;23(12):1400–1406.
11. Moskowitz IP, et al. The T-Box transcription factor Tbx5 is required for the patterning and maturation of the murine cardiac conduction system. *Development*. 2004;131(16):4107–4116.
12. Bruneau BG, et al. Chamber-specific cardiac expression of Tbx5 and heart defects in Holt-Oram syndrome. *Dev Biol*. 1999;211(1):100–108.
13. Pfeufer A, et al. Genome-wide association study of PR interval. *Nat Genet*. 2010;42(2):153–159.
14. Holm H, et al. Several common variants modulate heart rate, PR interval and QRS duration. *Nat Genet*. 2010;42(2):117–122.
15. Tan N, et al. Weighted gene coexpression network analysis of human left atrial tissue identifies gene modules associated with atrial fibrillation. *Circ Cardiovasc Genet*. 2013;6(4):362–371.
16. Zang X, et al. SNP rs3825214 in TBX5 is associated with lone atrial fibrillation in Chinese Han population. *PLoS One*. 2013;8(5):e64966.
17. Nadadur RD, et al. Pitx2 modulates a Tbx5-dependent gene regulatory network to maintain atrial rhythm. *Sci Transl Med*. 2016;8(354):354ra115.
18. Oka T, et al. Cardiac-specific deletion of Gata4

reveals its requirement for hypertrophy, compensation, and myocyte viability. *Circ Res*. 2006;98(6):837–845.
19. Bisping E, et al. Gata4 is required for maintenance of postnatal cardiac function and protection from pressure overload-induced heart failure. *Proc Natl Acad Sci U S A*. 2006;103(39):14471–14476.
20. Heineke J, et al. Cardiomyocyte GATA4 functions as a stress-responsive regulator of angiogenesis in the murine heart. *J Clin Invest*. 2007;117(11):3198–3210.
21. Yang YQ, et al. GATA4 loss-of-function mutations in familial atrial fibrillation. *Clin Chim Acta*. 2011;412(19–20):1825–1830.
22. Jiang JQ, Shen FF, Fang WY, Liu X, Yang YQ. Novel GATA4 mutations in lone atrial fibrillation. *Int J Mol Med*. 2011;28(6):1025–1032.
23. Posch MG, et al. Mutations in the cardiac transcription factor GATA4 in patients with lone atrial fibrillation. *Eur J Med Genet*. 2010;53(4):201–203.
24. Boldt LH, et al. Mutational analysis of the PITX2 and NKX2-5 genes in patients with idiopathic atrial fibrillation. *Int J Cardiol*. 2010;145(2):316–317.
25. Huang RT, Xue S, Xu YJ, Zhou M, Yang YQ. A novel NKX2.5 loss-of-function mutation responsible for familial atrial fibrillation. *Int J Mol Med*. 2013;31(5):1119–1126.
26. Xie WH, et al. Prevalence and spectrum of Nkx2.5 mutations associated with idiopathic atrial fibrillation. *Clinics (Sao Paulo)*. 2013;68(6):777–784.
27. Briggs LE, et al. Perinatal loss of Nkx2-5 results in rapid conduction and contraction defects. *Circ Res*. 2008;103(6):580–590.
28. Pashmforoush M, et al. Nkx2-5 pathways and congenital heart disease; loss of ventricular myocyte lineage specification leads to progressive cardiomyopathy and complete heart block. *Cell*. 2004;117(3):373–386.
29. Chung IM, Rajakumar G. Genetics of congenital heart defects: the NKX2-5 gene, a key player. *Genes (Basel)*. 2016;7(2):E6.
30. Jay PY, et al. Nkx2-5 mutation causes anatomic hypoplasia of the cardiac conduction system. *J Clin Invest*. 2004;113(8):1130–1137.
31. Jay PY, et al. Haploinsufficiency of the cardiac transcription factor Nkx2-5 variably affects the expression of putative target genes. *FASEB J*. 2005;19(11):1495–1497.
32. Furtado MB, et al. A novel conditional mouse model for Nkx2-5 reveals transcriptional regulation of cardiac ion channels. *Differentiation*. 2016;91(1–3):29–41.
33. Garg V, et al. GATA4 mutations cause human congenital heart defects and reveal an interaction with TBX5. *Nature*. 2003;424(6947):443–447.
34. Ang YS, et al. Disease model of GATA4 mutation reveals transcription factor cooperativity in human cardiogenesis. *Cell*. 2016;167(7):1734–1749.e22.
35. Maitra M, et al. Interaction of Gata4 and Gata6 with Tbx5 is critical for normal cardiac development. *Dev Biol*. 2009;326(2):368–377.
36. Nadeau M, et al. An endocardial pathway involving Tbx5, Gata4, and Nos3 required for atrial septum formation. *Proc Natl Acad Sci U S A*. 2010;107(45):19356–19361.
37. Stefanovic S, Barnett P, van Duijvenboden K, Weber D, Gessler M, Christoffels VM. GATA-dependent regulatory switches establish atrioventricular canal specificity during heart development. *Nat Commun*. 2014;5:3680.
38. Takeuchi JK, et al. Tbx5 specifies the left/right ventricles and ventricular septum position during cardiogenesis. *Development*. 2003;130(24):5953–5964.
39. Ding B, et al. p204 is required for the differentiation of P19 murine embryonal carcinoma cells to beating cardiac myocytes: its expression is activated by the cardiac Gata4, Nkx2.5, and Tbx5 proteins. *J Biol Chem*. 2006;281(21):14882–14892.
40. Linhares VL, et al. Transcriptional regulation of the murine Connexin40 promoter by cardiac factors Nkx2-5, GATA4 and Tbx5. *Cardiovasc Res*. 2004;64(3):402–411.
41. Misra C, Chang SW, Basu M, Huang N, Garg V. Disruption of myocardial Gata4 and Tbx5 results in defects in cardiomyocyte proliferation and atrioventricular septation. *Hum Mol Genet*. 2014;23(19):5025–5035.
42. Kasahara H, Benson DW. Biochemical analyses of eight NKX2.5 homeodomain missense mutations causing atrioventricular block and cardiac anomalies. *Cardiovasc Res*. 2004;64(1):40–51.
43. Bruneau BG, et al. A murine model of Holt-Oram syndrome defines roles of the T-box transcription factor Tbx5 in cardiogenesis and disease. *Cell*. 2001;106(6):709–721.
44. Moskowitz IP, et al. A molecular pathway including Id2, Tbx5, and Nkx2-5 required for cardiac conduction system development. *Cell*. 2007;129(7):1365–1376.
45. Postma AV, et al. A gain-of-function TBX5 mutation is associated with atypical Holt-Oram syndrome and paroxysmal atrial fibrillation. *Circ Res*. 2008;102(11):1433–1442.
46. Luna-Zurita L, et al. Complex interdependence regulates heterotypic transcription factor distribution and coordinates cardiogenesis. *Cell*. 2016;164(5):999–1014.
47. Mahida S. Transcription factors and atrial fibrillation. *Cardiovasc Res*. 2014;101(2):194–202.
48. Pradhan L, et al. Intermolecular interactions of cardiac transcription factors NKX2.5 and TBX5. *Biochemistry*. 2016;55(12):1702–1710.
49. Molkentin JD, Lin Q, Duncan SA, Olson EN. Requirement of the transcription factor GATA4 for heart tube formation and ventral morphogenesis. *Genes Dev*. 1997;11(8):1061–1072.
50. Kuo CT, et al. GATA4 transcription factor is required for ventral morphogenesis and heart tube formation. *Genes Dev*. 1997;11(8):1048–1060.
51. Lyons I, et al. Myogenic and morphogenetic defects in the heart tubes of murine embryos lacking the homeo box gene Nkx2-5. *Genes Dev*. 1995;9(13):1654–1666.
52. Watt AJ, Battle MA, Li J, Duncan SA. GATA4 is essential for formation of the proepicardium and regulates cardiogenesis. *Proc Natl Acad Sci U S A*. 2004;101(34):12573–12578.
53. He A, Kong SW, Ma Q, Pu WT. Co-occupancy by multiple cardiac transcription factors identifies transcriptional enhancers active in heart. *Proc Natl Acad Sci U S A*. 2011;108(14):5632–5637.
54. Yang XH, et al. Transcription-factor-dependent enhancer transcription defines a gene regulatory network for cardiac rhythm. *Elife*. 2017;6:e31683.
55. White SM, Constantin PE, Claycomb WC. Cardiac physiology at the cellular level: use of cultured HL-1 cardiomyocytes for studies of cardiac muscle cell structure and function. *Am J Physiol Heart Circ Physiol*. 2004;286(3):H823–H829.
56. Nattel S, Dobrev D. Electrophysiological and molecular mechanisms of paroxysmal atrial fibrillation. *Nat Rev Cardiol*. 2016;13(10):575–590.
57. Christophersen IE, et al. Large-scale analyses of common and rare variants identify 12 new loci associated with atrial fibrillation. *Nat Genet*. 2017;49(6):946–952.
58. Voigt N, et al. Cellular and molecular mechanisms of atrial arrhythmogenesis in patients with paroxysmal atrial fibrillation. *Circulation*. 2014;129(2):145–156.
59. Voigt N, et al. Enhanced sarcoplasmic reticulum Ca^{2+} leak and increased Na^{+}-Ca^{2+} exchanger function underlie delayed afterdepolarizations in patients with chronic atrial fibrillation. *Circulation*. 2012;125(17):2059–2070.
60. Nattel S, Shiroshita-Takeshita A, Brundel BJ, Rivard L. Mechanisms of atrial fibrillation: lessons from animal models. *Prog Cardiovasc Dis*. 2005;48(1):9–28.
61. Dai W, et al. A calcium transport mechanism for atrial fibrillation in Tbx5-mutant mice. *Elife*. 2019;8:e41814.
62. Liu GS, et al. A novel human R25C-phospholamban mutation is associated with super-inhibition of calcium cycling and ventricular arrhythmia. *Cardiovasc Res*. 2015;107(1):164–174.
63. Schmitt JP, et al. Dilated cardiomyopathy and heart failure caused by a mutation in phospholamban. *Science*. 2003;299(5611):1410–1413.
64. van der Zwaag PA, et al. Phospholamban R14del mutation in patients diagnosed with dilated cardiomyopathy or arrhythmogenic right ventricular cardiomyopathy: evidence supporting the concept of arrhythmogenic cardiomyopathy. *Eur J Heart Fail*. 2012;14(11):1199–1207.
65. Hayward C, Banner NR, Morley-Smith A, Lyon AR, Harding SE. The current and future landscape of SERCA gene therapy for heart failure: a clinical perspective. *Hum Gene Ther*. 2015;26(5):293–304.
66. Sikkel MB, Hayward C, MacLeod KT, Harding SE, Lyon AR. SERCA2a gene therapy in heart failure: an anti-arrhythmic positive inotrope. *Br J Pharmacol*. 2014;171(1):38–54.
67. Morihara H, et al. Phospholamban inhibition by a single dose of locked nucleic acid antisense oligonucleotide improves cardiac contractility in pressure overload-induced systolic dysfunction in mice. *J Cardiovasc Pharmacol Ther*. 2017;22(3):273–282.
68. Hoshijima M, et al. Chronic suppression of heart-failure progression by a pseudophosphorylated mutant of phospholamban via in vivo cardiac rAAV gene delivery. *Nat Med*. 2002;8(8):864–871.
69. Kaneko M, Hashikami K, Yamamoto S, Matsumoto H, Nishimoto T. Phospholamban ablation using CRISPR/Cas9 system improves mortality in a murine heart failure model. *PLoS One*. 2016;11(12):e0168486.
70. Zhu Y, et al. Tbx5-dependent pathway regulating diastolic function in congenital heart disease. *Proc Natl Acad Sci U S A*. 2008;105(14):5519–5524.

71. Roberts JD. Noncoding genetic variation and gene expression: deciphering the molecular drivers of genome-wide association study signals in atrial fibrillation. *Circ Genom Precis Med*. 2018;11(3):e002109.
72. Iyer LM, et al. A context-specific cardiac β-catenin and GATA4 interaction influences TCF7L2 occupancy and remodels chromatin driving disease progression in the adult heart. *Nucleic Acids Res*. 2018;46(6):2850–2867.
73. Ventura A, et al. Restoration of p53 function leads to tumour regression in vivo. *Nature*. 2007;445(7128):661–665.
74. Luo W, et al. Targeted ablation of the phospholamban gene is associated with markedly enhanced myocardial contractility and loss of beta-agonist stimulation. *Circ Res*. 1994;75(3):401–409.
75. Wheeler MT, Allikian MJ, Heydemann A, Hadhazy M, Zarnegar S, McNally EM. Smooth muscle cell-extrinsic vascular spasm arises from cardiomyocyte degeneration in sarcoglycan-deficient cardiomyopathy. *J Clin Invest*. 2004;113(5):668–675.
76. Arnolds DE, et al. TBX5 drives Scn5a expression to regulate cardiac conduction system function. *J Clin Invest*. 2012;122(7):2509–2518.